

Cathode region of a transitory discharge in CO₂. I. Theory of the cathode region

P. Bayle, J. Vacquie, and M. Bayle

Laboratoire de Génie Electrique, Université Paul Sabatier, 118 Route de Narbonne, 31062 Toulouse Cédex, France

(Received 12 December 1985)

The inception of the cathode region of a transitory discharge in CO₂ is studied by means of a spatio-temporal second-order hydrodynamic model (continuity equations for electrons and ions, momentum and energy equations for electrons). The electric field is calculated by Poisson equation. This first paper deals particularly with the formalism developed for this study. A term-to-term analysis of the equations allows the characterization of the physical mechanisms governing each part of the cathode region. The balance between the electric field acting as a source of energy and the elastic and inelastic collisions acting as loss processes is studied. The whole collective phenomena in the discharge (diffusion and work of electronic pressure strength which are made explicit by the gradients in the equations) play a regulating role in relation to the energy-gain or -loss processes. In a place where the field action is significant, i.e., in the cathode fall, they contribute to reduce this action and are energy- and velocity-loss processes for the electrons, whereas, in the negative glow, they compensate for the quasinull action of the electric field, and thus they are the only processes maintaining the energy and the velocity of the electrons in this zone. The cathode-fall–negative-glow transition zone is defined as the zone where the action of the energetic collective phenomena (total diffusion, work of electron pressure) is reversed.

I. INTRODUCTION

One of the most significant problems in gas discharges is the discontinuity in the current flow due to the electrodes. On the anode side, the electrode plays the role of a generally passive absorber for electrons, whereas the cathode acts both as a positive-ion absorber and as an electron producer, leading to a more complex situation. Townsend's breakdown criterium shows that the cathode determines the extinction, the persistency, or the outburst of a stationary discharge. Thus, the cathode processes (as an electron source) play a significant role in the discharge. Moreover, the cathode region is the only region with a high electric field gradient in stationary discharges (whereas in transitory discharges it shares this peculiarity with the ionizing wave fronts). However, though fundamental, this part of the discharge, particularly in its transitory form leading to the inception of the glow discharge, is not very well known.

In fact, its weak spatial expansion reduces the experimental studies. The description of the cathode region of a glow discharge can be found in Von Engel,¹ Badareu and Popescu,² Champann,³ Francis,⁴ Allis,⁵ and Emeleus.^{6,7} The cathode region shows two main zones: the cathode fall (CF) and the negative glow (NG). The cathode fall is defined as the region between the cathode and zero-field value point, and is characterized by a significant electric field gradient whereas the negative glow is a weak, nearly null electric field region.

Warren⁸ gave field measurements in glow discharges at a pressure ranging from 0.03 to 1.0 Torr in flowing gases (helium, nitrogen, . . .) with currents ranging from 0.1 to 10 mA. The length of the cathode-fall region decreases as the current increases and the electric field shape decreases

linearly in a first approach. Warren found that the ionization in the cathode-fall region is low until it increases abruptly on the cathode side of the negative glow, very near the position in the discharge where the field first approaches zero.

Theoretical analysis found in the literature mainly deal with the cathode-fall region and are equilibrium studies. The first studies settled analytic formalisms. Warren⁹ gave a partial analytic solution for the cathode region which predicts the form of the variation of the field with position, pressure, and current. This solution depends upon the different laws governing the motion of positive ions in the different parts of the discharge.

Neuringer¹⁰ improved these calculations by an analytic investigation of the cathode-fall region in high-voltage, low-current gas discharges. Explicit expressions for the variations of the electric field, the voltage drop, the charge density, the Joule heating, and the cathode-fall thickness were obtained as functions of pressure, current density, and distance from the cathode.

However, the nonlinearity of the equations, linked to the phenomena intricacy, leads to a necessary numeric treatment of these equations to obtain a complete analysis of the spatio-temporal inception and development of the cathode region. A zero-order model roughly gives analytic relations between the electric field, the cathode fall, the reduced current J/p^2 , and the cathode-fall length. Ward^{11,12} and Nahemow, Wainfan, and Ward¹³ made the first studies of the evolution of the cathode region in an argon discharge by means of the numerical resolution of an equilibrium first-order model, based on the continuity equations and on Poisson equation. This model led to a quasilinearly decreasing electric field distribution, with a maximum electric field value on the cathode.

Davies and Evans¹⁴ put forth an improved numerical method leading to the spatial variations of the electronic current and of the electric field. A numerical solution was given by Evdokimov *et al.*¹⁵ from the continuity and Poisson equations for singly charged ions and electrons, in a gas discharge excited by electrons. Narrow anode and cathode voltage-drop sections were shown to be formed in a discharge in nitrogen at atmospheric pressure. The cathode drop is much larger than the anode one. The field at the cathode increases and the length of the cathode drop decreases as the densities of ions and electrons in the gap increase. Morrow,¹⁶ in the theory of negative corona in oxygen, studied the development of the current and the distributions of charge carriers and electric field. The theory was based on the numerical solution of Poisson's equation in conjunction with the continuity equations for electrons, positive and negative ions. He found that as the discharge develops, a dense plasma forms near the cathode, leading to strong space-charge distortion of the field. A prominent cathode-fall region is formed immediately adjacent to the cathode, an almost-zero-field region is formed. Furthermore, the cathode-fall region becomes reduced to such a short distance that insignificant current is produced from this region.

Nevertheless, because of the strong gradients taking place in this region, the electrons are no longer in equilibrium with the electric field and this leads to a nonequilibrium modeling of the cathode region. The analysis of this phenomenon can be made either by a microscopic analysis of the discharge (Monte Carlo or Boltzmann methods) or by a macroscopic method. The electron behavior in the cathode-fall region of a glow discharge in helium has been analyzed using a one-dimensional Monte Carlo method by Tran Ngoc An, Marode, and Johnson.¹⁷ They showed that the effective ionization coefficient has a very different spatial dependence from the one expected using the Townsend coefficient in the vicinity of the negative glow. Using a Monte Carlo method and a null-collision technique based on determination of the kinetic energy increase between two collisions, Boeuf and Marode¹⁸ studied the steady-state behavior of the cathode region of a glow discharge in helium and gave the spatial variations of energy and angular electron distribution functions and the spatial variations of the macroscopic electron parameters. Ohuchi and Kubota¹⁹ simulated the cathode region (CF and NG) in helium by the Monte Carlo method in a three-dimensional space using the constant time-step technique. They showed that the electron density increased in front of the cathode due to the backscattering effect and that the mean energy of electrons decreased in the negative glow, taking into account the reflection of electrons from the anode. Lalau²⁰ studied the cathode-fall region of a steady-state glow discharge by a Boltzmann equation analysis and gave self-consistent results for the space-charge electric field and for the spatial evolution of electron and ion densities. In conclusion, it is obvious that the fundamental problem in the cathode region is the relative strong field gradient and the secondary electrons.

The secondary electrons ejected by the cathode have temperatures nearly independent from the local conditions of the gaseous medium into which they enter. These elec-

trons are ejected in a zone of high spatio-temporal gradients with a high electric field value. They multiply in conditions far from the equilibrium conditions for which the classic first-order hydrodynamic models of the discharge were established. Obviously, quasihomogeneity and quasistationarity no longer exist. The electron multiplication is no longer governed by the electric field alone but also by the energetic balance due to all the collisional and transport processes arising in the gas. Thus, such a complex situation calls for an analysis of the phenomena by means of second-order models able to show the energetic variations of the electrons.

The purpose of this work was to study the inception and the development of the cathode region (CF and NG) in a transitory discharge in CO₂ by means of a two-order model based on the electronic and ionic continuity equations, the electronic momentum equation, and the electronic energy equation. This macroscopic analysis gives the behavior of electrons and ions and allows one to follow the spatio-temporal evolution of collective phenomena inducing the nonequilibrium between the electrons and the electric field. This model is very well adapted to the study of nonequilibrium situations such as those induced by strong spatio-temporal gradients of the cathode region. The collective phenomena (linked to strong gradients in the field variation and in energy density) are shown to play a major role in the inception of the cathode-fall region, and the ionization mechanisms which take place and lead to a maximum in the electron multiplication only at the transition zone between the cathode fall and the negative glow are described.

II. HYDRODYNAMIC MODEL OF THE CATHODE REGION

A. General formalism of nonequilibrium transitory discharges

The formalism hereafter developed is an extension of that proposed by Abbas and Bayle²¹ and by Bayle and Cornebois.²² It is based on the hydrodynamics of slightly ionized gases. However, apart from the fact that the discharge studied here evolves in an electronegative gas (whereas in Refs. 21 and 22 the gas was nitrogen), particular care was devoted to the formulation of the equation of electronic momentum transfer which can no longer be used in its simplified form.

1. Fundamental hypothesis

The discharge evolves in a passive, cold, static, and uniform CO₂ gas. The discharge is supposed to consist of electrons and positive ions created by collisional ionization. In a first approach, the nature of the negative ions created by attachment is not significant but the part taken by the negative ions in the net space-charge density can be conclusive. So, only one kind of negative ions whose creation rate is deduced from the total attachment cross section is considered. The volume recombination processes are neglected. In order to be specified, the ionization and attachment terms need a microscopic hypothesis on

the electron distribution function, which is assumed to be isotropic and Maxwellian (see Appendix on distribution function). The negative-ion mobility is nearly the same as that of positive ions (their mobility is 100 times less than the electron mobility). The mobility of the positive CO_2^+ ions is very low as regards the electron mobility but they cannot be neglected, as in the cathode region and principally in the cathode-fall region, their density is high compared to the electron density and they play a significant role in the total current density. Thus, it is assumed that the CO_2^+ ions move with a drift velocity function of the electric field but the diffusion effect of the ions is neglected. The positive and negative ions are in equilibrium with the electric field, so their movement is well described by the continuity equations. Because of the strong spatio-temporal gradients taking place in this zone, the electrons cannot be considered in equilibrium with the electric field. Their energy can be very different from the energy calculated in an equilibrium situation, using a value of the electric field equal to the local electric field. So, the electron energy is deduced from the energy equation settled in a previous paper.²² This implies that all the collisional interaction operators involved in the macroscopic equations will be explicitly expressed as a function of this energy. Thus, the nonequilibrium between the electrons and the electric field implies the use of density, momentum- and energy-transfer equations to describe electron movement.

2. Mathematic nonequilibrium model of the cathode region

a. Continuity equations. The continuity equation for electrons is

$$\frac{\partial n_e}{\partial t} + \frac{\partial(n_e u_e)}{\partial x} = S_{\text{ion}} - S_{\text{att}}, \quad (1)$$

for the negative ions

$$\frac{\partial n^-}{\partial t} + \frac{\partial(n^- u^-)}{\partial x} = S_{\text{att}}, \quad (2)$$

and for the positive ions

$$\frac{\partial n_+}{\partial t} - \frac{\partial(n_+ u_+)}{\partial x} = S_{\text{ion}}, \quad (3)$$

with n_e the electron density, u_e the electron velocity, n^- the negative-ion density, n_+ the positive-ion density, u_+ the positive-ion velocity, and u^- the negative-ion velocity. S_{ion} and S_{att} , respectively the ionization and the attachment source terms, are the number of electrons created or attached in 1 sec in the volume unit. They must be expressed as a function of the electron temperature T_e , of the electron density n_e , and of the neutral gas density N ;

$$S_{\text{ion}}(T_e, n_e, N) = N n_e \int_0^\infty \sigma_{\text{ion}}(\epsilon) w(\epsilon) f(\epsilon) d\epsilon, \quad (4)$$

with $\sigma_{\text{ion}}(\epsilon)$ ionization cross section and $f(\epsilon)$ Maxwellian electron distribution function

$$S_{\text{att}}(T_e, n_e, N) = N n_e \int_0^\infty \sigma_{\text{att}}(\epsilon) w(\epsilon) f(\epsilon) d\epsilon, \quad (5)$$

with $\sigma_{\text{att}}(\epsilon)$ attachment cross section.

b. Momentum transfer equation. In the case of the cathode region, the situation is even more complex than that analyzed in Ref. 22 as the simplified equation no longer fits its use. As a matter of fact, near the cathode there are two reasons for nonequilibrium. On the one hand, as for ionizing waves, nonequilibrium arises from the strong spatio-temporal gradients of density and field, and on the other hand, it arises from the discontinuity due to the cathode surface. Secondary electrons are ejected from the cathode (by ionic or photonic impact) with a mean velocity entirely different from that of the electrons in the gas. This introduces a nonequilibrium new condition which implies a great care in the local electron velocity calculation, particularly in the zone adjoining the cathode, which is the greatest field gradient zone. In this area, these nonequilibrium effects amplify each other and an electron ejected from the cathode has to move up to a point of the cathode fall, before its properties become simply functions of the phenomena occurring in the gas. The momentum-transfer equation, deduced from the Boltzmann equation, can be written as

$$\frac{\partial}{\partial t}(m_e n_e u_e) + \frac{\partial}{\partial x}(n_e T_e) + \frac{\partial}{\partial x}(m_e n_e u_e^2) - n_e e E = (\nabla^e + \nabla^i) m_e w_e, \quad (6)$$

with m_e the electron mass, e the electron charge, E the electric field, and $(\nabla^e + \nabla^i) m_e w_e$ is the symbolic operator of momentum transfer by elastic and inelastic collisions. Taking into account Eq. (1), Eq. (6) can be written as

$$\frac{\partial u_e}{\partial t} + u_e \frac{\partial u_e}{\partial x} = \frac{e}{m_e} E - \frac{e}{m_e n_e} \frac{\partial(n_e T_e)}{\partial x} - u_e \frac{S_{\text{ion}} - S_{\text{att}}}{n_e} - \frac{(\nabla^e + \nabla^i) m_e w_e}{m_e n_e}. \quad (7)$$

Thus, the electron velocity appears as the result of a balance between the velocity gain due to the electric field (first term of the equation), and a velocity loss due to collisions (last term). The middle terms show the role of collective phenomena of the discharge on the electrons. The second term of the right-hand side (rhs) is the total diffusion velocity, a function of the energy density gradient. This diffusion velocity depends on the geometric and energetic properties of the discharge. The use of the total diffusion defined here can lead to completely different results compared with those obtained with the classic diffusion. Particularly, the total diffusion can be direct or reverse depending on the electron temperature gradient. (A study of the total diffusion was made in the first step of this modeling by Abbas and Bayle²¹ to study the inception of an electron shock wave.) The role played by the total diffusion on the inception of the negative glow and of the cathode-fall region is studied in the next section. The third term of the rhs is the momentum necessary for the electrons created by ionization (with a null-assumed mean velocity and energy) to reach the mean local velocity.

c. Electron energy transfer equation. The electron energy transfer equation, deduced from the Boltzmann equation is

$$\begin{aligned} & \frac{3}{2} \left(\frac{\partial T_e}{\partial t} + u_e \frac{\partial T_e}{\partial x} \right) \\ &= u_e E - \frac{1}{n_e} \frac{\partial(n_e T_e u_e)}{\partial x} - \frac{3}{2} T_e (S_{\text{ion}} - S_{\text{att}}) \\ & \quad - \frac{1}{n_e} (\nabla^e + \nabla^i) \frac{1}{2} m_e w_e^2, \end{aligned} \quad (8)$$

where $(\nabla^e + \nabla^i) \frac{1}{2} m_e w_e^2$ is the symbolic operator of energy transfer by elastic and inelastic collisions.

The electron energy gain under the electric field [first term of the rhs of Eq. (8)] is balanced by the collisional losses (last term of the rhs whereas the second term of the rhs, which is positive or negative according to the discharge structure, acts as a regulator for energy-gain or -loss processes. This term is essential in the transition between the cathode-fall and the negative-glow region and in the existence of the negative glow itself. It represents the role of the collective phenomena (apart from the space-charge field effect) by which the geometric and energetic properties of the electron cloud maintain (or at the opposite reduce) the mean electron energy in the different zones of the discharge. The third term of the rhs is the mean energy necessary with which to provide the electrons, so that they reach the mean local temperature of the electron cloud.

B. Specification of the operators of momentum and energy transfer equations in nonequilibrium discharges

The basic idea, as settled by Abbas and Bayle²¹ and by Bayle and Cornebois²² to the symbolic operator $(\nabla^e + \nabla^i) \frac{1}{2} m_e w_e^2$ is enlarged to the operator $(\nabla^e + \nabla^i) m_e w_e$. In the macroscopic modeling, these operators may be specified globally in the following way.

a. Energy transfer operator. In an equilibrium situation (stationary and uniform discharges), the energy provided by the electric field is completely used to heat the created electrons and to compensate for the energy lost by collisions. Thus, the electron energy is stationary and uniform. So

$$n_e E_s v_d = \frac{3}{2} T_{\text{es}} (S_{\text{ion}} - S_{\text{att}}) + (\nabla^e + \nabla^i) \frac{1}{2} m_e w_e^2, \quad (9)$$

T_{es} being the equilibrium static temperature, v_d the drift velocity, and E_s the uniform and stationary electric field. In an equilibrium situation, the electron energy only depends on the electric field value.

If the relations

$$T_{\text{es}} = f(E_s) \quad (10)$$

or

$$E_s = \psi(T_{\text{es}})$$

are known, and if the ionization and attachment source terms are expressed as function of the static electron temperature, this can be expressed as a function of the static electron temperature,

$$\begin{aligned} (\nabla^e + \nabla^i) \frac{1}{2} m_e w_e^2 &= n_e \psi(T_{\text{es}}) v_d [\psi(T_{\text{es}})] \\ & \quad - \frac{3}{2} T_{\text{es}} [S_{\text{ion}}(T_{\text{es}}) - S_{\text{att}}(T_{\text{es}})]. \end{aligned} \quad (11)$$

In a nonequilibrium situation (transitory and nonuniform discharges), the energy-transfer equation (8) shows that the electron energy is not only a function of the local electric field but also of the geometric and energetic properties of the whole discharge. The dynamic electron temperature is deduced from Eq. (8). We assume that the same formal dependence of the macroscopic terms with temperature is maintained, thus the extrapolation of this formal dependence of the energy losses versus temperature, by replacing the static temperature T_{es} by the dynamic one T_e in Eq. (11), leads to

$$\begin{aligned} (\nabla^e + \nabla^i) \frac{1}{2} m_e w_e^2 &= n_e \psi(T_e) v_d [\psi(T_e)] \\ & \quad - \frac{3}{2} T_e [S_{\text{ion}}(T_e) - S_{\text{att}}(T_e)]. \end{aligned} \quad (12)$$

The energy equation is

$$\begin{aligned} \frac{3}{2} \left(\frac{\partial T_e}{\partial t} + u_e \frac{\partial T_e}{\partial x} \right) &= E u_e - \frac{1}{n_e} \frac{\partial(n_e T_e u_e)}{\partial x} \\ & \quad - \psi(T_e) v_d [\psi(T_e)]. \end{aligned} \quad (13)$$

b. Momentum transfer equation. In the equilibrium situation, the electronic mobility is linked to the elastic collision frequency (nearly equal to the total collision frequency) by the relation $\mu_e = e / (m_e \nu_e)$, and μ_e (or ν_e) depends only on the reduced electric field E/N and thus the momentum-transfer operator is a function of the reduced electric field E/N (or of the static temperature).

In order to explicitly define the momentum-transfer operator $(\nabla^e + \nabla^i) m_e w_e$ in a nonequilibrium situation, we assume that the same formal dependence of the macroscopic interaction terms is maintained and that this leads to the same formulation, taking into account the fact that the collision frequency is no longer a function of the reduced electric field but of the dynamic electron temperature, deduced from the energy equation. The following relations for the momentum-transfer operator are deduced. In an equilibrium situation,

$$(\nabla^e + \nabla^i) m_e w_e = n_e m_e u_e \nu_e(E/N), \quad (14)$$

with

$$\nu_e(E/N) = \frac{e}{m_e} \frac{1}{\mu_e(E/N)}$$

or

$$\nu_e(T_{\text{es}}) = \frac{e}{m_e} \frac{1}{\mu_e \left[\frac{\psi(T_{\text{es}})}{N} \right]}, \quad (15)$$

where $\mu_e(E/N)$ is the electron mobility. In a nonequilibrium situation, the same formal dependency is used but the collision frequency is a function of the dynamic temperature

$$(\nabla^e + \nabla^i) m_e w_e = n_e m_e u_e \nu_e(T_e), \quad (16)$$

with

$$v_e(T_e) = \frac{e}{m_e} \frac{1}{\mu_e[\psi(T_e)/N]},$$

where $\mu_e(T_e)$ is the mobility expressed as a function of the dynamic temperature. So Eq. (7) can be written as

$$\frac{\partial u_e}{\partial t} + u_e \frac{\partial u_e}{\partial x} = \frac{e}{m} \left[E - \frac{1}{n_e} \frac{\partial(n_e T_e)}{\partial x} \right] - u_e \frac{S_{\text{ion}} - S_{\text{att}}}{n_e} - u_e v_e[\psi(T_e)]. \quad (17)$$

C. Source term and macroscopic coefficients

1. Ionization and attachment source terms

The ionization and attachment cross sections used in relations (4) and (5) to calculate the source terms are from Kucukarpaci and Lucas.²³ Their shapes have been fitted

by simple mathematical functions to give an analytic formulation of the source terms. The ionization cross section is

$$N\sigma_{\text{ion}}(\epsilon) = K_1(\epsilon - W_i)\Delta(\epsilon - W_i), \quad (18)$$

with $K_1 = 0.126 \text{ cm}^{-1} \text{ eV}^{-1}$, $W_i = 13.3 \text{ eV}$, and Δ is the Heaviside distribution. The total attachment cross section is

$$N\sigma_{\text{att}}(\epsilon) = K_2[\Delta(\epsilon - W_{A1}) - \Delta(\epsilon - W_{A2})] + K_3[\Delta(\epsilon - W_{A3}) - \Delta(\epsilon - W_{A4})], \quad (19)$$

with $K_2 = 0.5 \times 10^{-2} \text{ cm}^{-1} \text{ eV}^{-1}$, $K_3 = 1.6 \times 10^{-2} \text{ cm}^{-1} \text{ eV}^{-1}$, $W_{A1} = 4.2 \text{ eV}$, $W_{A2} = 4.6 \text{ eV}$, $W_{A3} = 8 \text{ eV}$, and $W_{A4} = 8.4 \text{ eV}$. The source terms at 293 K can be written as

$$S_{\text{ion}} = 1.16 \times 10^{-8} n_e N \sqrt{T_e} e^{-13.3/T_e} \left[1 + \frac{2T_e}{13.3} \right], \quad (20)$$

$$S_{\text{att}} = 3.163 \times 10^{-11} n_e N \sqrt{T_e} \left[\left[1 + \frac{8}{T_e} \right] e^{-8/T_e} - \left[1 + \frac{8.4}{T_e} \right] e^{-8.4/T_e} \right] + 9.897 \times 10^{-12} n_e N \sqrt{T_e} \left[\left[1 + \frac{4.2}{T_e} \right] e^{-4.2/T_e} - \left[1 + \frac{4.6}{T_e} \right] e^{-4.6/T_e} \right], \quad (21)$$

where N is the neutral density (cm^{-3}), T_e the electron temperature in eV, and S_{ion} and S_{att} in $\text{cm}^{-3} \text{ s}^{-1}$. The cross sections are adjusted so that, in an equilibrium situation, the following relation is verified:

$$S_{\text{ion}} - S_{\text{att}} = \frac{\lambda}{N} N n_e v_d, \quad (22)$$

where λ/N is the apparent ionization coefficient from Dutton²⁴ including all the gain and loss processes.

2. Drift velocities

a. *For electrons.* The electron drift velocity is deduced from Gallagher *et al.*²⁵ At 293 K with v_d in cm s^{-1} and E/N in Td (townsend) it is

$$\begin{aligned} E/N \geq 1153 \text{ Td}, \quad v_d &= 8.291 \times 10^5 (E/N)^{0.581}, \\ 667 \leq E/N < 1153 \text{ Td}, \quad v_d &= 3.28 \times 10^7 + 1.477 \times 10^4 (E/N), \\ 23 \leq E/N < 667 \text{ Td}, \quad v_d &= 1.174 \times 10^6 + 1.606 \times 10^6 (E/N)^2, \\ E/N < 23 \text{ Td}, \quad v_d &= 8.803 \times 10^4 (E/N)^{1.47}. \end{aligned} \quad (23)$$

b. *For positive ions.* The positive-ion drift velocity is deduced from Saporoschenko²⁶ at 293 K as

$$\begin{aligned} E/N \geq 425 \text{ Td}, \quad v_+ &= 5.971 \times 10^3 (E/N)^{1/2}, \\ E/N < 425 \text{ Td}, \quad v_+ &= 264 (E/N). \end{aligned} \quad (24)$$

c. *For negative ions.* Their mobility is assumed equal to the positive-ion mobility.

3. Relations between the electric field and the electronic temperature at equilibrium

These relations are deduced from Kucukarpaci and Lucas²³ at 293 K as

$$\begin{aligned} E/N \leq 66 \text{ Td}, \quad T_e \text{ (eV)} &= 2.824 \times 10^{-2} (E/N) - 1.08 \times 10^{-5}, \\ E/N > 66 \text{ Td}, \quad T_e \text{ (eV)} &= 0.3621 + [3.988 \times 10^{-2} (E/N) - 0.2488]^{1/2}. \end{aligned} \quad (25)$$

D. Electric field

For the formalism presented to be self-consistent, it needs to associate to the equations of hydrodynamics of slightly ionized gas an equation dealing with the electric field evolution. We assume that the discharge analyzed is spread on the cathode compared to the spatial expansion of the cathode region. In these conditions, the mono-dimensional Poisson equation gives a good representation of the resulting field,

$$\frac{\partial E}{\partial x} = \frac{e}{\epsilon_0}(n_+ - n_e - n^-). \quad (26)$$

This set of equations with initial and boundary conditions is solved by the well-known characteristics method.

III. DEFINITION OF THE INITIAL AND BOUNDARY CONDITIONS

A. Initial conditions

The study of the nonequilibrium stage of a transitory discharge depends on the knowledge of the foregoing equilibrium stage. The two-order modeling, taking into account the energetic processes moving electrons away from equilibrium, can be solved only by numerical schemes implying severe limitations on the spatial and temporal computation intervals. Complete analysis of the discharge by means of such a modeling requires too much computation time. So the first stages of the discharge are simulated by zero- or first-order models until these models are no longer valid.

The initial conditions of our study are defined using the experimental conditions of Cobine,²⁷ Ivanchenko and Shepelenko,²⁸ and Francis.⁴ Table I gives the initial conditions of the discharge. V and d are, respectively, the cathode-fall voltage and length.

As the determining parameter of the cathode region is the electric field, an *a priori* spatial repartition is taken, from which the spatial repartitions of the electronic and ionic densities are deduced by zero-order relationships. The field is assumed to vary linearly through the cathode-fall region from $E = 1.4 \times 10^4$ V cm⁻¹ at the cathode to $E = 3.4 \times 10^2$ V cm⁻¹ at the end of the cathode fall. The electronic profile is defined as

$$n_e(x) = n_e(0) \exp(\langle \lambda \rangle x), \quad (27)$$

with $\langle \lambda \rangle = 117.9$ cm⁻¹ and $n_e(0) = 10^{-11}$ C cm⁻³. If we notice that the attachment coefficient is weak in front of the ionization coefficient, the negative ions may be neglected (with a zero-order approximation), so the positive ions may be deduced from the Poisson equation as

$$n_+(x) = \epsilon_0 \frac{\partial E}{\partial x} + n_e(x). \quad (28)$$

Figure 1 represents the initial conditions from which the computation begins. The computational program adjusts these data in the frame of a two-order modeling and after less than 1 ns delay (necessary to adapt to inevitably approximate initial conditions) gives a correct representation of the discharge evolution.

B. Boundary conditions

The current density on the cathode is given by

$$J_e(0,t) = \gamma_+ J_+(0,t) + \gamma_{ph} \int_0^d S_{exc}(x,t) dx. \quad (29)$$

Secondary electrons are ejected by ionic and photonic impacts (with probability respectively equal to γ_+ and γ_{ph}). The mean values of γ_+ and γ_{ph} have been assessed to be equal to

$$\gamma_+ = 5 \times 10^{-2}, \quad \gamma_{ph} = 10^{-4}.$$

The excitation source term S_{exc} is evaluated in the same way as the ionization and attachment source terms. The excitation cross sections of CO₂, given by Kucukarpaci and Lucas,²³ are fitted by the following relations:

$$\begin{aligned} N\sigma_{exc}(\epsilon) = & C_1 \delta(\epsilon - W_1) + C_2 \delta(\epsilon - W_2) \\ & + C_3 (\epsilon - W_3) \Delta(\epsilon - W_3) \\ & + C_4 (\epsilon - W_4) \Delta(\epsilon - W_4), \end{aligned} \quad (30)$$

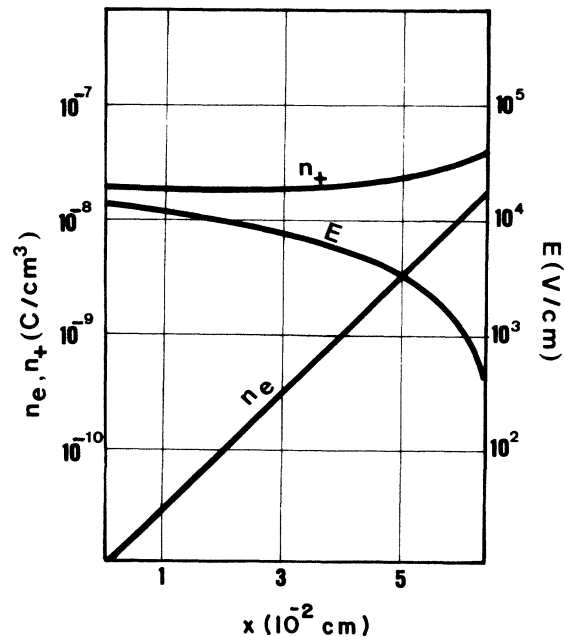


FIG. 1. Initial conditions. E is the electric field profile, n_e electronic density profile, and n_+ positive-ion density profile. To be easily compared with results on Fig. 2 the electric field is drawn in semilogarithmic scale. (The abscissa is the distance from the cathode.)

TABLE I. Initial conditions.

Gas: CO ₂	
$p = 20$ Torr	$I = 4.61 \times 10^{-3}$ A
$V = 437$ V	$J/p^2 = 1.63 \times 10^{-4}$ A/cm ² Torr ²
$pd = 1.28$ Torr cm	$E_{cathode}/N = 2.125 \times 10^3$ Td (293 K)

δ is the Dirac function, Δ the Heaviside distribution, and

$$C_1 = 1.5 \text{ cm}^{-1} \text{ eV}^{-1}, \quad W_1 = 3.1 \text{ eV},$$

$$C_2 = 0.9 \text{ cm}^{-1} \text{ eV}^{-1}, \quad W_2 = 7.0 \text{ eV},$$

$$C_3 = 0.22 \text{ cm}^{-1} \text{ eV}^{-1}, \quad W_3 = 10.5 \text{ eV},$$

$$C_4 = 2.6 \times 10^{-2} \text{ cm}^{-1} \text{ eV}^{-1}, \quad W_4 = 11.5 \text{ eV}.$$

S_{exc} , the excitation source term at 293 K is

$$S_{\text{exc}}(T_e, n_e, N) = N n_e \int_0^\infty \sigma_{\text{exc}}(\epsilon) w(\epsilon) f(\epsilon) d\epsilon, \quad (31)$$

$$S_{\text{exc}}(T_e, n_e, N) = N n_e \left[C_5 \sqrt{T_e} \left[1 + \frac{2T_e}{10.5} \right] e^{-10.5/T_e} + C_6 \sqrt{T_e} \left[1 + \frac{2T_e}{11.5} \right] e^{-11.5/T_e} + \frac{C_7}{\sqrt{T_e}} e^{-7/T_e} + \frac{C_8}{\sqrt{T_e}} e^{-3.1/T_e} \right], \quad (32)$$

with

$$C_5 = 9.593 \times 10^{-9}, \quad C_6 = 5.094 \times 10^{-9},$$

$$C_7 = 1.245 \times 10^{-8}, \quad C_8 = 9.186 \times 10^{-9}.$$

The two-order model is an energetic model. It is thus necessary to define a mean temperature for the secondary electrons ejected by the cathode, their velocity being deduced from $\epsilon_e = \frac{1}{2} m_e v_e^2$. It is generally assumed that the mean energy of secondary electrons lies between 0 and 20 eV (Von Engel,¹ Boeuf and Marode¹⁸). Different values of this ejection energy are checked ($T_e = 0.5, 1, 2, 5,$ and 10 eV) and the response of the secondary electrons to the electric field is studied. All the figures of this first paper

are obtained with a temperature of emitted electrons equal to 5 eV. On the anode side boundary, we assume that the positive-ion density is given by

$$n_+(d, t + \Delta t) = n_+(d, t) + S_{\text{ion}}(T_e, n_e, N) \Delta t. \quad (33)$$

IV. INCEPTION OF THE CATHODE REGION

A. Description of the spatial properties of the cathode region

Starting from the above-defined initial conditions, the inception of the cathode region is studied as a function of time. Figure 2 represents the cathode region, 13 ns after

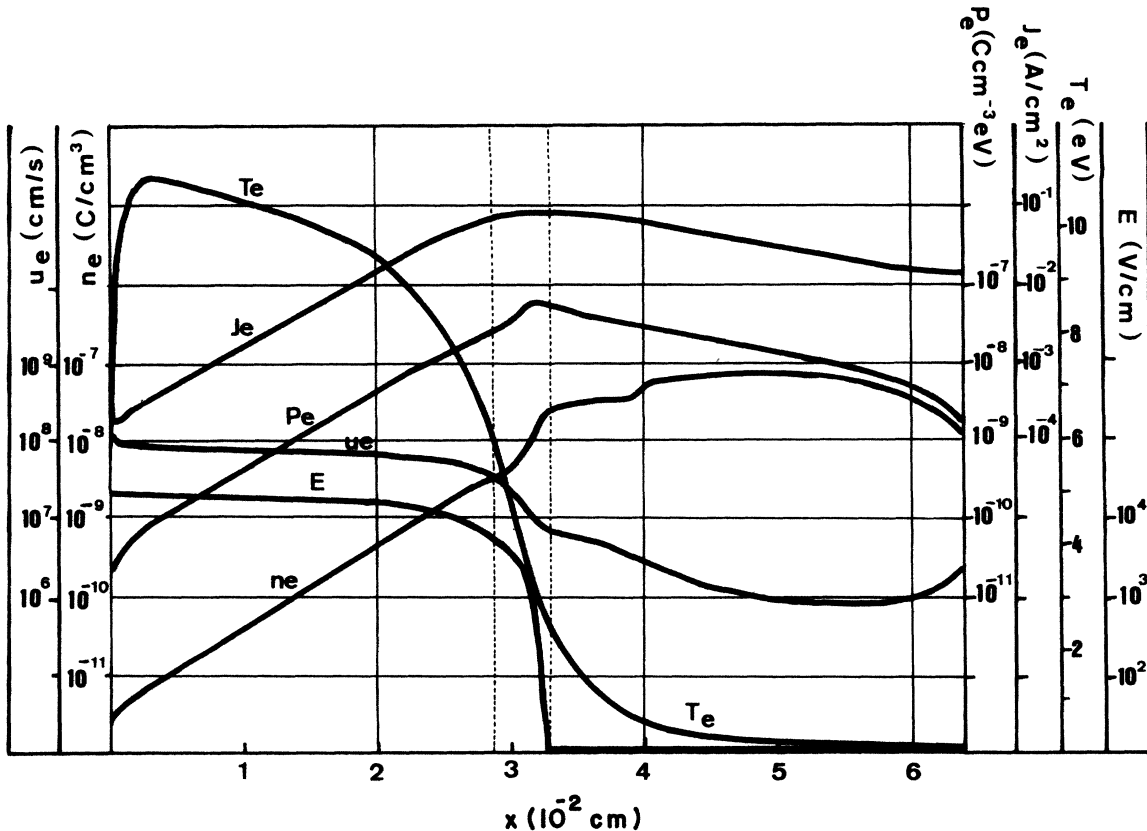


FIG. 2. Spatial evolution of the different macroscopic parameters in the discharge at $t = 13$ ns. T_e (eV) is the electron temperature, E (V cm^{-1}) electric field, $P_e = n_e T_e$ electron pressure, u_e electron velocity, n_e electron density, and J_e electron current density.

the initial conditions. The field gradient is no longer uniform and two different zones can be distinguished. The first one, characterized by a strong electric field, which decreases from the cathode, corresponds to what is generally called the "cathode-fall region," and the second one, with a very weak (nearly null) electric field can be defined as the "negative glow."

The cathode fall is characterized by a high electron temperature. The connection between a high electric field and a high electron temperature gives rise to strong transport phenomena while the electronic multiplication gradually increases the electron density from the cathode to the boundary between CF and NG.

The negative-glow is characterized by a low electron temperature and a very weak electric field. It is necessary to notice that the transport is weak but not null. The drift velocity no longer intervenes in the electron velocity which is principally governed by the diffusion phenomena linked to the energy gradient. The transition zone between the CF and the NG shows special properties linked to the field and energy density gradients. In this zone, the electric field gradients are the strongest and most of the cathode fall occurs. The terms $\partial(n_e T_e)/\partial x$ and $\partial(n_e T_e u_e)/\partial x$ from the momentum and energy equations change their signs. This means that the collective phenomena action (for example, total diffusion) is reversed. This inversion of collective phenomena induces very different properties in the CF and in NG. Particularly, this explains why the electron velocity is not null in the negative glow in spite of a nearly null electric field. But as the negative field is weak, the electron multiplication is weak

and the NG appears as a zone where electrons issued of the cathode-fall region gather.

The inception and the development of the cathode-fall region and negative-glow region are the results of the double action of transport phenomena and of multiplication phenomena, the function of the electron temperature. It is necessary, in order to understand the spatio-temporal evolution of the cathode region, to analyze the role of the different processes on the electron velocity and temperature.

B. Electron velocity

The electron velocity is the result of a balance between a velocity gain due to the electric field action and a velocity loss due to collisions, whereas the diffusion (the electron pressure gradient) acts like a regulator. Figure 3 shows the part these different processes (drift under electric field action, diffusion by energy gradient, collisions) play in the electron velocity evolution and in the inception of the different zones of the cathode region. The result for both the velocity gains and losses are each different in the cathode-fall region and in the negative-glow region.

In the cathode-fall region, the velocity gain greatly prevails. In this high electric field zone, where electrons are strongly accelerated, the transport phenomenon is highest. The loss occurs principally from collisions. The total diffusion slows the velocity gain and decreases the field action. Moreover, a part of the gain in momentum is used to raise the velocity of the electrons created (whose mean velocity is supposed to be null at the creation) up to the

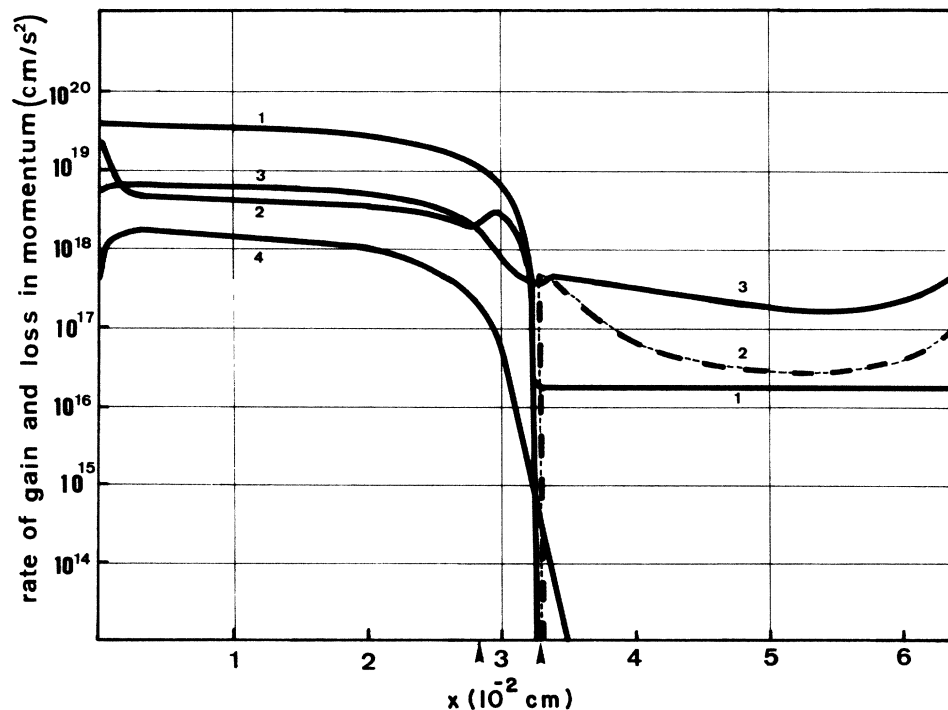


FIG. 3. Comparison between the spatial evolution of the different terms of the momentum equation at $t = 13$ ns. The dotted lines are used for negative values. (1) $(e/m_e)E$, (2) $(e/m_e)(1/n_e)[\partial(n_e T_e)/\partial x]$, (3) $v[\psi(T_e)]u_e$, (4) $(1/n_e)(S_{\text{ion}} - S_{\text{att}})u_e$.

mean local velocity of the electron swarm.

In the transition zone between the cathode-fall region and the negative-glow region (delimited by two arrows on Fig. 3), the drift due to the electric field gradually vanishes. The electron movement is no longer governed by the electric field, but by the diffusion processes that supply the electrons with almost all of their velocity.

In the negative-glow region, as the electric field is very weak, the drift velocity is weak and the electrons movement is the result of two actions: the collisions (loss of energy for the electrons) and the collective phenomena, i.e., the effect of total diffusion (gain of velocity for the electrons). This total diffusion velocity expresses the influence of the energetic structure of the discharge on its own evolution. Due to a feedback effect, this total diffusion effect reduces the electron velocity in the cathode-fall region where the electric field (and thus the drift velocity) is high, whereas in the negative-glow region [where the term $\partial(n_e T_e)/\partial x$ changes its sign] the diffusion effect maintains the velocity. This effect plays relatively a more significant role if the electric field is weak and an absolutely more significant role if the heterogeneity of the discharge is strong. The relative significance of the different terms of the momentum equation is shown in Figs. 4 and 5.

Figure 6 compares the total electron velocity [solution of Eq. (7)] to the drift velocity and to the diffusion velocity [second term of rhs of Eq. (7)]. In the transition zone, the diffusion velocity balances the drift velocity loss which becomes more pronounced in the negative glow. At both ends of the cathode-fall region, the diffusion is opposed in the most significant way to the electric field action to stabilize the total electron velocity leading, respectively, to a stabilization of the electrons issued from the cathode and to an acceleration of the negative-glow in-

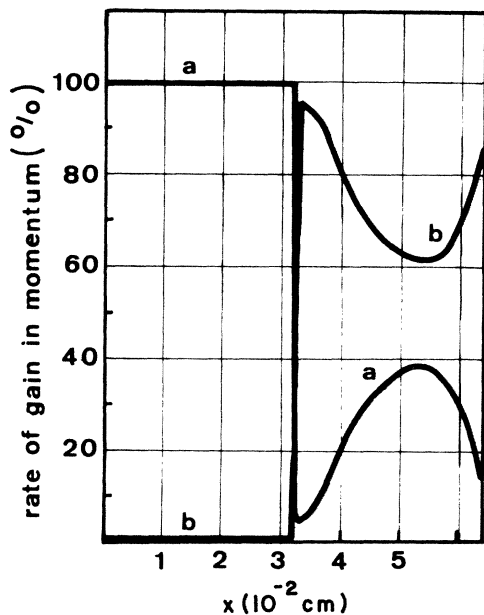


FIG. 4. Rate of gain in momentum induced by the different terms of the momentum equation (a) $(e/m_e)E$, (b) $(e/m_e)(1/n_e)[\partial(n_e T_e)/\partial x]$.

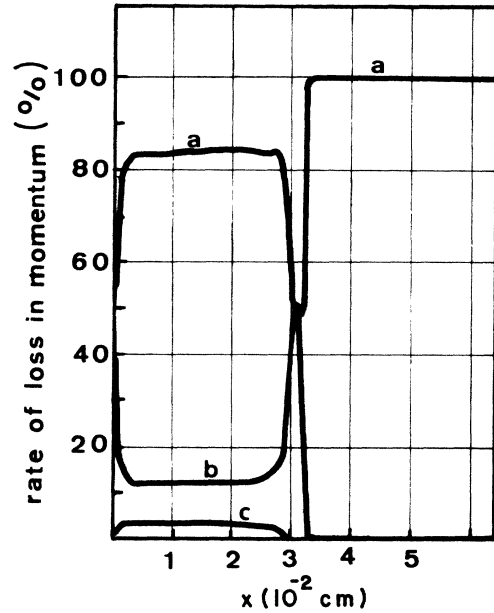


FIG. 5. Rate of loss in momentum induced by the different terms of the momentum equation (a) $v[\psi(T_e)]u_e$, (b) $(e/m_e)(1/n_e)[\partial(n_e T_e)/\partial x]$, (c) $[(S_{ion} - S_{att})/n_e]u_e$.

ception. The diffusion velocity acts as a stabilizing process in the modification of the electron velocity. Of course, the role of the collisions always reduces the electron velocity. The losses by collision play a significant role in the negative-glow region and a less significant role (compared to the electric field action) in the cathode-fall region.

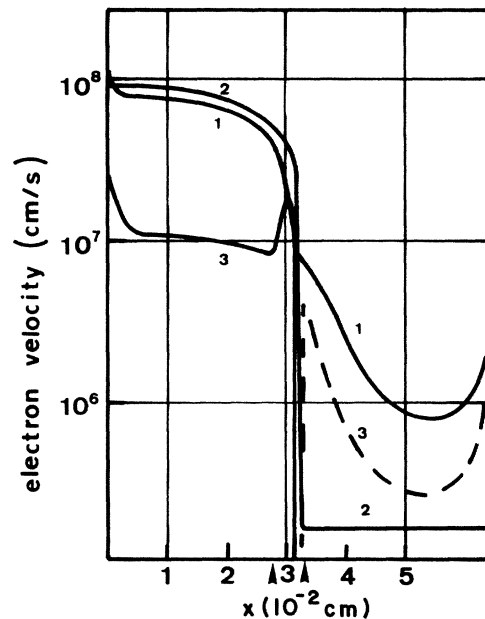


FIG. 6. Comparison between the total electron velocity (1), the diffusion velocity (3), and the drift velocity (2) $t=13$ ns (dashed lines for negative values).

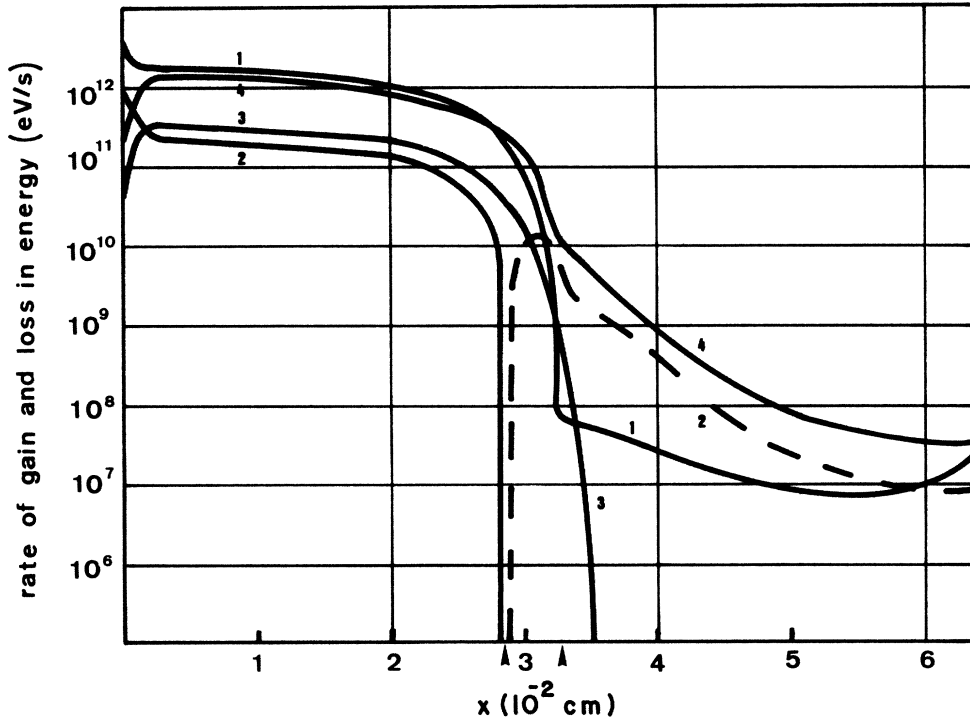


FIG. 7. Comparison between the different terms of the energy equation, $t=13$ ns (dashed lines for negative values). (1) $u_e E$, (2) $(1/n_e)[\partial(n_e T_e u_e)/\partial x]$, (3) $(1/n_e)[\frac{3}{2} T_e (S_{\text{ion}} - S_{\text{att}})]$, (4) $(1/n_e)(\nabla^e + \nabla^i) \frac{1}{2} m_e u_e^2$.

C. Electron temperature

Figure 7 shows how the different terms of the energy equation (8), and thus the different processes they

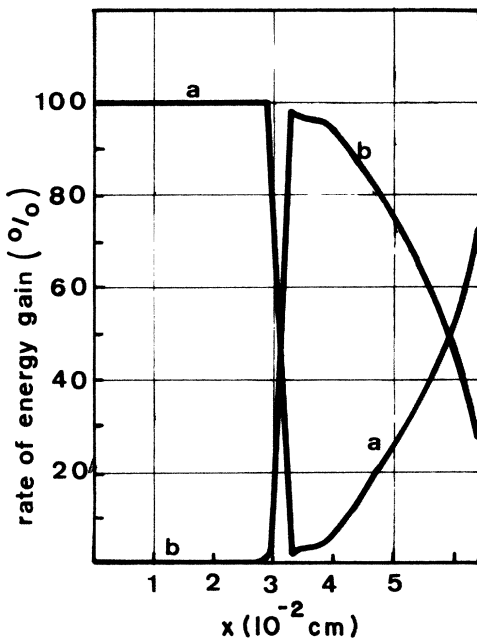


FIG. 8. Rate of energy gain induced by the different terms of the energy equation, $t=13$ ns. (a) $u_e E$, (b) $(1/n_e)[\partial(n_e T_e u_e)/\partial x]$.

represent, intervene in the electron temperature evolution. The division of the cathode region in two different zones is induced by different processes stepping in, which vary greatly from one point of the cathode region to another. Near the cathode, in the cathode-fall region, all the gain and loss processes are strong, whereas they are weak in the negative glow region. All over the cathode region, the elastic and inelastic collisions (curve 4 of Fig. 7) are the most significant loss processes. Their role in the final balance between the different processes depends on the electric field heating. In the cathode-fall region, the high electric field gives rise to a high electron heating and the electrons accumulate energy. A significant part of the energy provided by the electric field is eventually used to raise the temperature of the electrons ejected from the cathode to the mean local temperature of the electron swarm. The work of the electron pressure (which represents the action of the collective phenomena linked to the discharge structure) is opposed to the electron heating in this zone. In the negative glow, the processes are reversed. The nearly null electric field induces a nearly null electron heating. But the term representing the work of the electron pressure changes its sign. It thus plays the role of a source term in the energy equation and it represents the only gain process for the electrons. In the same way as for velocity, the electrons keep enough energy in the negative glow by a diffusion process. In the transition zone, the collision losses are stronger than the electron heating process and the work of the electron pressure changes its sign. The relative significance of each loss and gain process is shown on Figs. 8 and 9.

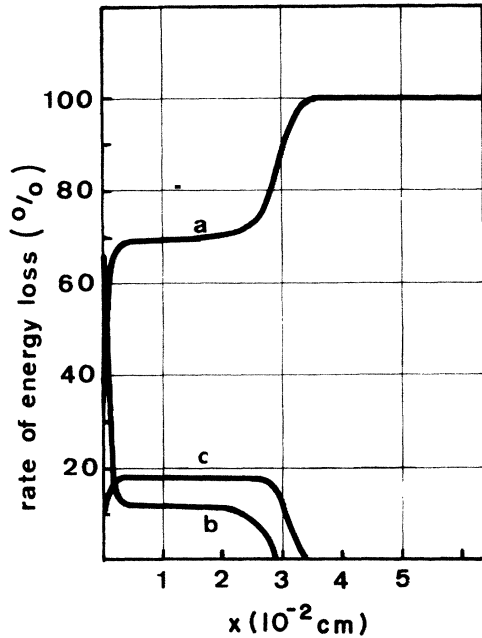


FIG. 9. Rate of energy loss induced by the different terms of the energy equation. (a) $(1/n_e)(\nabla^e + \nabla^i)\frac{1}{2}m_e w_e^2$, (b) $(1/n_e)[\partial(n_e T_e u_e)/\partial x]$, (c) $\frac{3}{2}T_e[(S_{\text{ion}} - S_{\text{att}})/n_e]$.

V. CONCLUSION

The setting of a macroscopic formalism giving explicit formulations of the interaction operators in the momentum and energy equations and the ionization, attachment and excitation source terms in the continuity equations as function of the electron temperature, makes a study of the inception and the development of the cathode region in a CO_2 discharge possible.

The term-by-term analysis of the equations allows a characterization of the relative role of the physical processes in each zone. The inception of the cathode region is the result of a balance between the action of the electric field acting as an energy source, and of the collective phenomena occurring in the discharge acting as a regulator process.

In the CF, the electrons gain energy under the field action, whereas the diffusion process and the loss due to collisions limit this gain in energy and velocity. In the NG, the diffusion effects play an active role and maintain the electron energy and velocity.

The transition zone is defined as the place where the collective phenomena change their signs. It makes the transition between a high electric field region to a nearly

null electric field region.

The nonequilibrium between the electrons and the electric field is obvious on the electron velocity and temperature. The drift velocity, the main component of the velocity in the CF, is null in the transition zone, whereas in the NG, the electron velocity is mainly due to diffusion effects.

APPENDIX: REMARK ON THE DISTRIBUTION FUNCTION

A macroscopic formalism is necessarily based on an *a priori* choice of the distribution function, and this choice is often very awkward. In fact, there is a lack of information on distribution function in the cathode region of a CO_2 discharge, the only information existing dealing with a helium discharge. The information on distribution function in the cathode region of a helium discharge is experimental and theoretical.

The experimental results of Gibbs and Webb²⁹ in a near the negative glow of an abnormal discharge in helium show that three different components appear in the distribution function. The theoretical simulation works of Boeuf and Marode⁸ and of Ohuchi and Kubota⁷ on a discharge in helium gave slightly different results with only two electron groups. The distribution function shows a tail of high-energy electrons in the vicinity of the cathode, but this tail progressively vanishes toward the negative glow, where the distribution function goes back to a classic shape with only one maximum for low-energy electrons.

All these works deal with helium, an atomic gas whose elastic and inelastic cross sections are very different. There is no evidence that the behavior of the distribution function in a polyatomic gas, such as CO_2 , with comparable elastic and inelastic cross sections, would be the same. For CO_2 , the inelastic cross sections are more uniformly distributed in energy and so the electron energy-loss processes are more evenly distributed, leading to a certainly less pronounced departure from the Maxwellian (see Nighan³⁰).

However, it is necessary to point out that the choice of a Maxwellian distribution function, even if it appears as slightly different from the real distribution function of the discharge, allows one to give an analytic representation of the source terms (ionization, attachment, excitation). In the macroscopic model given in this paper, the choice of the distribution function does not influence in a fundamental manner the description of the collective phenomena (diffusion and transport) occurring in the discharge, which remains the main target of this study.

¹Von Engel, *Ionized Gases* (Oxford University Press, New York, 1965).

²E. Badareu, I. Popescu, *Gaz Ionisés-Décharges dans les gaz* (Dunod, Paris, 1965).

³B. Chapman, *Glow Discharge Processes* (Wiley, New York, 1980).

⁴G. Francis, *Ionization Phenomena in Gases* (Butterworths, Lon-

don, 1960).

⁵W. P. Allis, *Physica* **82C**, 43 (1976).

⁶K. G. Emeleus, *J. Phys. D* **14**, 2179 (1981).

⁷K. G. Emeleus, *J. Phys. D* **15**, 1543 (1981).

⁸R. Warren, *Phys. Rev. A* **98**, 1650 (1955).

⁹R. Warren, *Phys. Rev. A* **98**, 1658 (1955).

¹⁰J. L. Neuringer, *J. Appl. Phys.* **49**, 590 (1978).

- ¹¹A. L. Ward, *Phys. Rev.* **112**, 1852 (1958).
¹²A. L. Ward, *J. Appl. Phys.* **33**, 2789 (1962).
¹³M. Nahemow, M. Wainfan, and A. L. Ward, *Phys. Rev.* **137**, 56 (1964).
¹⁴A. J. Davies and C. J. Evans, *J. Phys. D* **13**, L161 (1980).
¹⁵O. B. Evdokimow, V. V. Kremnev, G. A. Mesyats, and V. B. Ponomarev, *Sov. Phys. Tech. Phys.* **18**, 1478 (1974).
¹⁶R. Morrow, *Phys. Rev. A* **32**, 1799 (1985).
¹⁷Tran Ngoc An, E. Marode, and P. C. Johnson, *J. Phys. D* **10**, 2317 (1977).
¹⁸J. P. Boeuf and E. Marode, *J. Phys. D* **15**, 2169 (1982).
¹⁹M. Ohuchi and T. Kubota, *J. Phys. D* **16**, 1705 (1983).
²⁰F. Lalau, Thèse de Spécialité No. 2876, Université de Paris—Sud, Orsay, 1981.
- ²¹I. Abbas and P. Bayle, *J. Phys. D* **14**, 649 (1981); **14**, 661 (1981).
²²P. Bayle and B. Cornebois, *Phys. Rev. A* **31**, 1046 (1985).
²³H. N. Kucukarpaci and J. Lucas, *J. Phys. D* **12**, 2123 (1979).
²⁴J. Dutton, *Phys. Chem. Ref. Data* **4**, 577 (1975).
²⁵J. W. Gallagher, E. C. Beaty, J. Dutton, and L. C. Pitchford, *J. Chem. Ref. Data* **12**, 109 (1983).
²⁶M. Saporoschenko, *Phys. Rev.* **8**, 1044 (1973).
²⁷J. D. Cobine, *Gaseous Conductors* (Dover, New York, 1958).
²⁸A. I. Ivanchenko and A. A. Shepelenko, *Teplofiz. Vys. Temp.* **20**, 636 (1982).
²⁹P. Gibb and C. E. Webb, *J. Phys. D* **10**, 299 (1977).
³⁰W. L. Nighan, *Phys. Rev. A* **2**, 1989 (1970).